IOPscience iopscience.iop.org

Home Search Collections Journals About Contact us My IOPscience

# Electron spin resonance observation of Si dangling-bond-type defects at the interface of (100) Si with ultrathin layers of $SiO_x$, $Al_2O_3$ and $ZrO_2$

This article has been downloaded from IOPscience. Please scroll down to see the full text article.

2001 J. Phys.: Condens. Matter 13 L673

(http://iopscience.iop.org/0953-8984/13/28/103)

View the table of contents for this issue, or go to the journal homepage for more

Download details:
IP Address: 171.66.16.226
The article was downloaded on 16/05/2010 at 13:56

Please note that terms and conditions apply.

INSTITUTE OF PHYSICS PUBLISHING JOURNAL OF PHYSICS: CONDENSED MATTER

J. Phys.: Condens. Matter **13** (2001) L673–L680 PII: S0953-8984(01)24481-6

**LETTER TO THE EDITOR**

# Electron spin resonance observation of Si dangling-bond-type defects at the interface of (100) Si with ultrathin layers of $SiO_x$, $Al_2O_3$ and $ZrO_2$

**A Stesmans and V V Afanas'ev**

Department of Physics, University of Leuven, 3001 Leuven, Belgium

Received 2 May 2001
Published 29 June 2001
Online at stacks.iop.org/JPhysCM/13/L673

**Abstract**

Paramagnetic point defects were probed by electron spin resonance in stacks of (100) Si with nm-thin $SiO_x$, $ZrO_2$ and $Al_2O_3$ layers. After photodesorption of passivating hydrogen (300 K; 8.48 eV), the Si dangling bond type interface centres $P_{bo}$, $P_{b1}$ appear as prominent defects at all (100) Si/dielectric interfaces, with $P_{bo}$ densities up to $\sim 6 \times 10^{12}$ cm$^{-2}$. This $P_{bo}$, $P_{b1}$ fingerprint, generally unique for the thermal (100) Si/$SiO_2$ interface, indicates that, while reassuring for the Si/$SiO_x$/$ZrO_2$ case, the as-deposited (100)Si/$Al_2O_3$ interface is basically Si/$SiO_2$-like. As probed by the $P_b$-type defects, the interfaces are under substantially enhanced stress, characteristic for low-temperature Si/$SiO_2$ growth. Standard quality thermal Si/$SiO_2$ interface properties, as exposed by the $P_b$-type defects (density $\sim 1 \times 10^{12}$ cm$^{-2}$), may be approached by appropriate mild annealing ($\sim$650 °C). This fact of a naturally present or possibility to establish a high quality (100) Si/$SiO_2$-type interface, with ultrathin $SiO_2$ interlayer, may be basic to successful application of high-$\kappa$ metal oxides in Si-based devices.

The incessant trend in down-scaling continuously reemphasizes the vital role of the gate dielectric in metal–oxide–silicon (MOS) devices. One implication of this drastic lateral scaling is that to maintain efficient signal transmission, compensation for the lost areal gate capacitance is mandatory, which may be realized by reducing the gate oxide thickness and/or enhancing the dielectric permittivity $\varepsilon = \kappa\varepsilon_0$. So far, thermal $SiO_2$—an insulator natural to Si—has served as unsurpassed gate dielectric with such unique and superb properties that stretching its usage as far as possible appears natural. Yet, with the projected $SiO_2$ thicknesses in the sub-2 nm range for the near future [1], the application of this foremost insulator in MOS devices faces fundamental limits such as excessive direct (tunnelling) leakage current, boron penetration, electron mobility degradation and reliability problems [1, 2]. This has stimulated enhanced research in replacing $SiO_2$ with an alternative layer of high dielectric constant ($\kappa$) for future MOS generations. The application of higher-$\kappa$ insulators should enable usage of thicker films of equivalent $SiO_2$ electrical thickness (EOT, defined as $d_{EOT} = d_{high\text{-}\kappa}\varepsilon_{SiO_2}/\varepsilon_{high\text{-}\kappa}$) with an expected reduction in leakage current and improved gate reliability.

 © 2001 IOP Publishing Ltd Printed in the UK 

The research enjoys accelerating interest [3, 4], with an immense arsenal of complementary high sensitivity analysing techniques being applied in conjunction to explore microstructural, compositional, and bonding chemistry aspects of ultrathin (sub-5 nm) high-$\kappa$ films on Si [5–8]. Applied techniques include medium-energy ion scattering (MEIS), high-resolution transmission electron microscopy (HRTEM), nuclear resonance profiling (NRP) and x-ray photoelectron and Auger spectroscopy. Also, using electrical techniques, such as capacitance–voltage ($C$–$V$) and current–voltage ($I$–$V$), the investigation of the electrical performance (transport, charge trapping, presence of detrimental electrically active interface traps) has received much attention [8–10]. Inherent to these methods, however, little is revealed about the atomic nature of crucial point defects related to or at the origin of observed electrical deficiencies. Yet, as amply documented for the $Si/SiO_2$ structure, point defects have been demonstrated or hinted as the origin of a realm of detrimental aspects, such as adverse interface traps, oxide fixed charge, irradiation-induced degradation, stress-induced leakage current and thermally induced oxide breakdown. A most vital issue is the quality of the c-Si/insulator interface, particularly as regards the presence of electrically active inherent defects [11]. So, analysing the likely altered interface situation in c-Si/alternative dielectric structures *vis-à-vis* standard c-$Si/SiO_2$ may appear of interest for advancing semiconductor device technology.

One intensely investigated alternative dielectric is $ZrO_2$ ($\kappa \sim 20$). Here, in a complementary approach, electron spin resonance (ESR)—the technique of choice for atomic identification of defects—is applied to stacks of ultrathin $SiO_x$ and $Al_2O_3$ films sandwiched between (100) Si and thin $ZrO_2$ layers, with the aim of providing atomic identification and quantification. The known characteristics of the amply studied $Si/SiO_2$ structure are used as a backdrop. Among other things, it is revealed that the ruling paramagnetic inherent interface defects in $Si/SiO_2$, i.e. $P_b$-type centres, also appear as major players at the interface of (100) Si with ultrathin $Al_2O_3$ and $SiO_x$ layers.

The $P_b$-type centres have received intense research interest (see, e.g. [11–14]). In short, these are mismatch-induced inherent point defects at the $Si/SiO_2$ interface, correlating with interface orientation. Three types are common [11]: $P_b$ (identified as $Si_3 \equiv Si^{\bullet}$) in (111) $Si/SiO_2$, and $P_{bo}$, $P_{b1}$ (a $\langle 211\rangle$-oriented $Si_3 \equiv Si^{\bullet}$ [15, 16]) in (100) $Si/SiO_2$. All three variants were shown to be trivalent Si centres, with $P_b$ and $P_{bo}$ demonstrated as chemically identical [17, 18] and both conclusively established as adverse electrical interface traps [13, 19]. For standard oxidation temperatures $T$ (800–960 °C), areal densities of physical defect sites (including both ESR active and inactive ones) of $[P_b] \sim 5 \times 10^{12}$ cm$^{-2}$ and $[P_{bo}]$, $[P_{b1}] \sim 1 \times 10^{12}$ cm$^{-2}$ are naturally incorporated [14, 20].

Samples studied were $Si/SiO_x/ZrO_2$ and $Si/Al_2O_3/ZrO_2$ stacks, prepared on low-doped one-side polished 8 inch (100) Si wafers (p type; $n_a \sim 10^{15}$ cm$^{-3}$; 0.8 mm thick) last cleaned in aqueous HF (5% by volume) prior to dielectric layer deposition. Uniform stoichiometric ultrathin layers of $Al_2O_3$ (~0.5–3 nm) and $ZrO_2$ (5–20 nm), as well as ultrathin $SiO_x$ layers, were deposited at 300 °C in an atomic layer chemical vapour deposition (ALCVD) reactor (hot-wall flow type F-450 reactor, ASM Microchemistry Ltd, Finland) using $Al(CH_3)_3$ and $H_2O$ and $ZrCl_4$ and $H_2O$ as precursors, respectively, at a pressure of ~1 Torr. The $SiO_x$ layers (~5 Å) were grown in $H_2O$ at 300 °C for 20 min. The ALCVD technique, with inherent thickness and uniformity control, allows the deposition of ultrathin dielectric layers with excellent step coverage and thickness uniformity; it attains nearly atomic layer accuracy. More details can be found elsewhere [8]. From these wafers, slices of $2 \times 9$ mm$^2$ main area, appropriate for ESR, were cut with their 9 mm edge along a $[0\bar{1}1]$ direction. After initial ESR diagnosis, some samples were submitted to mild annealing at ~650 °C in vacuum ($<4 \times 10^{-6}$ Torr) or dry $O_2$ (99.9995%; ~1.1 atm).

The interest in inserting interlayers ($Al_2O_3$, $SiO_x$) derives from various sides. On the basic

physics side, e.g., as to $ZrO_2$, one may try to improve on the much-reduced conduction band offset with respect to Si of $ZrO_2$ ($2.0 \pm 0.1$ eV) [21] as compared to $SiO_2$ ($3.15 \pm 0.05$ eV), in order to reduce Schottky emission leakage currents. On the chemical-manufacturing side, there is the influence of the growth base on the film deposition characteristics. Regarding ALCVD of $ZrO_2$ layers, it has been found that the nucleation on H-terminated last HF dipped (100) Si surfaces is inhibited [7], resulting in nonuniform and discontinuous films. However, after pregrowth of a thin thermal oxide, uniform $ZrO_2$ film growth is observed, with an abrupt interface between $SiO_2$ and $ZrO_2$. Finally, in a more general context, investigation of the impact of interlayers may be desirable in the light of the concern that fabrication of whatever Si/metal oxide structure may always be attendant, to a greater or lesser extent, with the occurrence, however thin, of some chemically intermixed transitional layer threatening the aimed 'ideal' abrupt transition.

It is a general property of paramagnetic point defects they are prone to ESR inactivation (at moderate temperatures) though binding with H, a phenomenon well known [12, 22] for the Si dangling-bond-type defects $P_b$, $P_{bo}$ and $P_{b1}$ at $Si/SiO_2$ interfaces (see also $E'$-type defects in $Si/SiO_2$ physics [23]). Hence, given the particular ALCVD fabrication technique (H-rich ambient), it is anticipated that most point defects will be left effectively passivated (invisible for ESR). In the case of $P_b$-type defects, the standard method to efficiently detach H is thermal treatment at elevated $T$ (typically $\sim$600 °C; $\sim$1 h). Clearly, however, such a step might irreversibly alter the initial physicochemical structure of interfaces and dielectric layers, with embedded defects, thus marring the study of the initial state. Rather than, as the preferred method, prior to ESR observations, samples were generally subjected to 8.48 eV VUV irradiation obtained from a Xe resonant discharge lamp (flux $5 \times 10^{14}$ cm$^{-2}$ s$^{-1}$; $\sim$5 min; 300 K) in air to photo-dissociate H-terminated dangling bonds [24] and/or possibly unveil non-ideal (strained, weak) bonding. The method has been demonstrated to be most efficient for both oxide and interface defects in $Si/SiO_2$. The front side interfaces and dielectric layers are found not to be affected by the VUV treatment, except for the ESR defect activation.

Conventional CW absorption-derivative K-band ($\sim$20.2 GHz) ESR analysis was carried out at 4.3 K under conditions of adiabatic slow passage [14]. The applied magnetic field $\boldsymbol{B}$ was rotated in the $(0\bar{1}1)$ Si substrate plane with $\varphi_B$, the angle of $\boldsymbol{B}$ with the [100] interface normal $\boldsymbol{n}$, varying in the range 0°–90° (accuracy $\sim$0.1°). Spin densities were determined relative to a comounted intensity marker through double numerical integration of the detected derivative-absorption spectra $\mathrm{d}P_\mu/\mathrm{d}B$, recorded in one trace. The attained absolute and relative accuracy is estimated at $\sim$10 and 5%, respectively. The backside of the samples was HF dipped immediately before starting ESR measurements. Typically, an ESR sample bundle comprised $\sim$10 slices.

Figure 1 shows ESR spectra observed at 4.3 K on $Si/Al_2O_3$ (0.5)/$ZrO_2$ (5 nm). As anticipated, only weak signals could be observed in the as-deposited state. However, signals do appear prominently upon VUV irradiation. For $\boldsymbol{B} \parallel \boldsymbol{n}$ (i.e. $\varphi_B = 0°$), two clear signals are observed: a prominent one at $g = 2.0059 \pm 0.0001$, with peak-to-peak width $\Delta B_{pp} = 9.7 \pm 0.4$ G, and a weaker one characterized by $g = 2.003\,75 \pm 0.0001$ and $\Delta B_{pp} = 3.75 \pm 0.2$ G, with spin densities ($S = \frac{1}{2}$) determined as $5.9 \pm 0.3$ and $(1.5 \pm 0.2) \times 10^{12}$ cm$^{-2}$, respectively (intensity ratio $R \sim 3.9$).

The signals exhibit distinct anisotropy, as evidenced by spectrum (b) in figure 1. These properties are reminiscent of the well known $P_{bo}$ and $P_{b1}$ centres at the thermal $Si/SiO_2$ interface. Field angular dependent measurements ($\boldsymbol{B}$ in the $(0\bar{1}1)$ plane) resulted in the $g$-map data shown in figure 2. The curves represent the various $g$ branches of the $P_{bo}$ and $P_{b1}$ centres as inferred from previous work [17] on conventional (100) $Si/SiO_2$, with principal $g$ values $g_\parallel = 2.001\,85$, $g_\perp 2.0081$ for $P_{bo}$ (axial symmetry; solid curves) and $g_1 = 2.005\,77$,

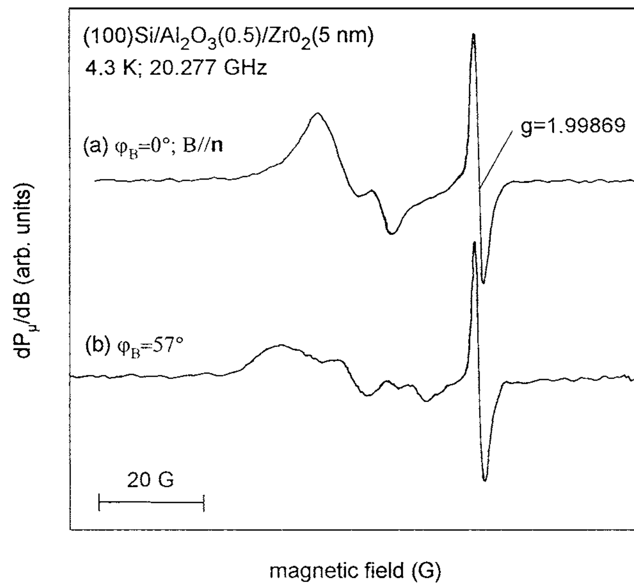


**Figure 1.** Derivative-absorption ESR spectra observed at 4.3 K for two directions of $\boldsymbol{B}$ in the $(0\bar{1}1)$ plane on a (100) $Si/Al_2O_3$ (0.5)/$ZrO_2$ (5 nm) stack, grown by the ALCVD method at 300 °C using $H_2O$, $Al(CH_3)_3$ and $ZrCl_4$ as precursors, after RT VUV irradiation (8.48 eV; ∼5 min) to detach H from passivated defects, clearly revealing the presence of $P_{bo}$, $P_{b1}$ defects at the $Si/Al_2O_3$ interface. The signal at $g = 1.998\,69$ stems from a comounted Si:P marker sample. The applied modulation field amplitude was 0.4 G, and incident $P_\mu \sim 2$ nW.

$g_2 = 2.007\,35$, $g_3 = 2.0022$ for $P_{b1}$ (monoclinic-I point symmetry; dotted curves). The agreement leaves little doubt about the $P_{bo}$, $P_{b1}$ origin of the signals. Also, the estimated relative signal (branch) intensities for the various equivalent defect orientations comply with the prescribed ones, i.e. 1:2:1 indicated on the figure, for both defect types. As is the case for $Si/SiO_2$, this strict crystallographic correlation with the Si substrate implies the defects pertain to the (100) $Si/Al_2O_3$ interface. Of course, there is also the second internal $Al_2O_3/ZrO_2$ interface. But the amorphous nature of both metal oxide films excludes involvement of the observed defects with this transition. This conclusion is affirmed by the study of simple (100) $Si/Al_2O_3$ (3 nm) ALCVD structures, exhibiting an identical $P_{bo}/P_{b1}$ pattern.

Similar observations were made on the (100) $Si/SiO_x$ (0.5)/$ZrO_2$ (5 nm) structure, i.e. observation of a prominent $P_{bo}$ signal and a weaker $P_{b1}$ signal, yet with two noticeable differences. First, as compared to the $Si/Al_2O_3$ (0.5)/$ZrO_2$ (5 nm) case, the signals are narrower, i.e. $\Delta B_{pp} = 6.8 \pm 0.4$ and $3.5 \pm 0.2$ G, for $P_{bo}$ and $P_{b1}$, respectively. Second, relative to the $P_{bo}$ signal (density $= 4.3 \times 10^{12}$ cm$^{-2}$), the $P_{b1}$ signal is weaker ($R \geqslant 9$). The observed linewidths may be compared with those observed in thermal $Si/SiO_2$ grown at $T > 900$ °C, given as $\Delta B_{pp} = 6.0 \pm 0.2$ and $3.3 \pm 0.2$ G for $P_{bo}$ and $P_{b1}$, respectively. It thus appears that as compared to standard $Si/SiO_2$, the linewidths observed in the structures here are broadened, the more so for the $Si/Al_2O_3$ (0.5)/$ZrO_2$ (5 nm) stack. Interestingly, as reported previously, this signature, i.e. presence of a strong $P_{bo}$ bath with strongly reduced $P_{b1}$ signal as compared to thermal $Si/SiO_2$ and broadened lines, is the one typical for thermal $Si/SiO_2$ interfaces grown at low $T$. This is illustrated in figure 3, showing an ESR spectrum ($\boldsymbol{B} \parallel \boldsymbol{n}$) from a (100) $Si/SiO_2$ entity grown at 260 °C (1 atm $O_2$; ∼160 min), with observed $P_{bo}$ density of $\sim 5 \times 10^{12}$ cm$^{-2}$ and $R \sim 8$, close to the values reported for the (100) $Si/SiO_x/ZrO_2$ entity.

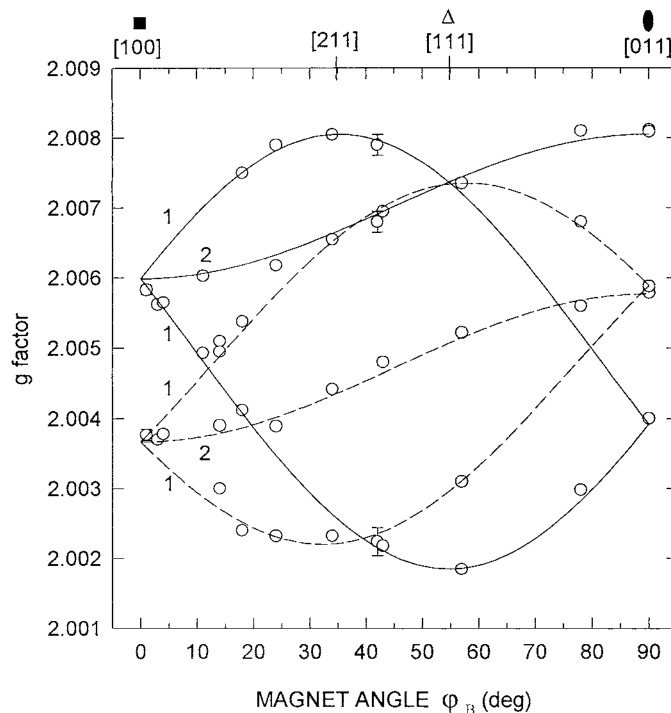


**Figure 2.** Angular dependence of the $g$ values of the resonances observed in an ALCVD-grown (100) $Si/Al_2O_3$ (0.5)/$ZrO_2$ (5 nm) structure after 300 s VUV irradiation at 300 °C for $\boldsymbol{B}$ rotating in the $(0\bar{1}1)$ plane. The curves represent the various $g$-map branches previously inferred for the $P_{bo}$ and $P_{b1}$ defects in standard thermal (100) $Si/SiO_2$, with principal values $g_\parallel = 2.001\,85$, $g_\perp = 2.0081$ for $P_{bo}$ (axial symmetry; solid curves) and $g_1 = 2.005\,77$, $g_2 = 2.007\,35$, $g_3 = 2.0022$ for $P_{b1}$ (monoclinic-I point symmetry; dotted curves). The exposed agreement demonstrates the observed signals to originate from $P_{bo}$, $P_{b1}$ defects residing at the $Si/Al_2O_3$ interface. The added numbers indicate expected relative branch intensities.

For comparison, also shown is a spectrum (a) from a more conventional $Si/SiO_2$ structure grown at ~800 °C.

Besides excessively broadened, it is also clear from figure 1 that the $P_{bo}$, $P_{b1}$ linewidth is field angle dependent, a well known characteristic first clearly quantified for $P_b$ in (111) $Si/SiO_2$ [25], and later also for $P_{bo}$ [17]. It refers to the presence of a spread in $g$, inferred as originating from mismatch (stress) induced local variations in the defect morphology over the various $P_{bo}$ sites [14]. The $\varphi_B$ dependence is predominantly ascribed to a strain-induced (supposedly) Gaussian distribution of spread $\sigma_{g\perp}$ in $g_\perp$. As to $P_b$, though not expected into first order [25, 26], it has been demonstrated there also exists a spread $\sigma_{g\parallel}$ in $g_\parallel$ [14], albeit significantly smaller than $\sigma_{g\perp}$. Hence, the excessive broadening of the $P_{bo}$ signal may be quantified in terms of variations in $g$ spread. Neglecting to a good approximation any $\sigma_{g\parallel}$ contribution, we obtain from an analysis along the lines outlined elsewhere [17], the values $\sigma_{g\perp}(P_{bo}) = 0.0011 \pm 0.0001$ and $0.001\,75 \pm 0.000\,15$ for the structures (100) $Si/SiO_x$ (0.5)/$ZrO_2$ (5 nm) and $Si/Al_2O_3/ZrO_2$, respectively. As compared to the value $\sigma_{g\perp} = 0.000\,95 \pm 0.000\,05$ for thermal (100) $Si/SiO_x$ [17], we thus find enhanced stress, in particular for the $Si/Al_2O_3$ interface.

Interestingly, upon annealing at ~650 °C in $O_2$, the Si/insulator interface in both the structures $Si/SiO_x/ZrO_2$ and $Si/Al_2O_3/ZrO_2$, as revealed by the specific the $P_{bo}$, $P_{b1}$ signature,

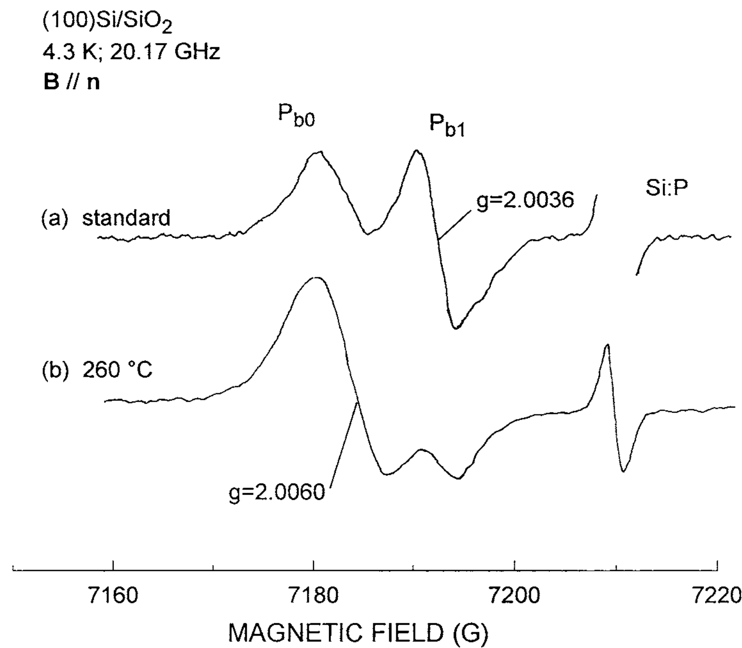


**Figure 3.** Curve (b): $P_b$, $P_{b1}$ ESR spectrum observed at 4.3 K for $\boldsymbol{B} \parallel$ [100] surface normal on thermal (100) $Si/SiO_2$ (260 °C; 1 atm $O_2$; ~160 min), with $[P_{bo}] \sim 5 \times 10^{12}$ $cm^{-2}$. Top spectrum: thermal (100)$Si/SiO_2$ grown at ~800 °C, with $P_{bo}$ and $P_{b1}$ spin densities inferred as ~1.6 and $1.9 \times 10^{12}$ $cm^{-2}$. Applied magnetic field modulation amplitude was 0.3 G; $P_\mu \sim 0.25$ nW.

reshapes to that of a standard high-quality thermal $Si/SiO_2$: the linewidths narrow to standard values, while densities reduce to standard low values of $\sim 1 \times 10^{12}$ $cm^{-2}$ for both defects. It is important to remark here that the appearance of the standard $P_{bo}$, $P_{b1}$ signature serves as a unique ESR criterion signalling a high-thermal-quality $Si/SiO_2$ interface; the interface of technological quality must exhibit its standard $P_{bo}$, $P_{b1}$ fingerprint.

The observations bear out various noteworthy aspects. (1) At the Si substrate/insulator interface in ALCVD-grown (100) $Si/SiO_x/ZrO_2$ and $Si/Al_2O_3/ZrO_2$ structures, the $P_{bo}$ and $P_{b1}$ defects—archetypal for a standard thermal (100) $Si/SiO_2$ interface—appear as predominant ESR-active centres. (2) While their occurrence might probably have been anticipated for the latter structure, their manifest presence at the (100) $Si/Al_2O_3$ interface reveals that, for an essential part, the basic nature of this interface is also (100) $Si/SiO_2$ type, from whereon the dielectric evolves to stoichiometric $Al_2O_3$. (3) As stated, the nominal thickness of the $SiO_x$ interlayer in the as-grown ALCVD (100) $Si/SiO_x/ZrO_2$ structure is 0.5 nm. Though ESR is little informative here, such a layer in the case of (100) $Si/Al_2O_3$ is likely thinner. In fact, it might just concern an oxygen monolayer case, as depicted in the particular ALCVD growth mechanism of $Al_2O_3$ using $Al(CH_3)_3$ and $H_2O$ precursors [27]. Here, the starting surface is an OH-passivated (Si–OH) Si surface, with the OH groups constituting the reactive sites for subsequent attack by trimethylaluminium molecules. As sketched, the interlayer just consists of a uniform singular Si–O–Al transitional layer (no direct Si–Al bonds), thus constituting a most ideal abrupt interface. But it is then probably inappropriate to refer to this as an $SiO_x$ layer. When grown on last HF cleaned (100) Si surfaces, abrupt interfaces are affirmed by combining NRP and MEIS depth profiling techniques [7]. Furthermore, the interface appears stable against rapid thermal annealing (RTA) in vacuum up

to 800 °C [5]. Physical abruptness of the $Si/Al_2O_3$ interface is also hinted from measurements of the effective image-force dielectric constant using internal photoemission spectroscopy [21]. Aiming low EOT, such abruptness is very favourable within the semiconductor device context, for any such layer should be kept as thin as possible.

However, the present ESR data would indicate the situation to be less than ideal. First, a substantial number of Si DB-type interface defects ($P_{bo}$, $P_{b1}$) ($\sim 7 \times 10^{12}$ cm$^{-2}$; that is, a fractional Si site occupancy of $\sim 1\%$ when referred to a singular (100) Si plane, about three to four times larger than in standard thermal (100) $Si/SiO_2$) is detected. Second, the observed $P_{bo}$, $P_{b1}$ ESR character (densities, line width) is the one typical for a (strained) low-temperature grown 'thermal' $Si/SiO_x$, the interface being under enhanced strain. It may then be hard to envision that a well ordered singular Si–O–Al transitional layer would exhibit such $Si/SiO_x$ character. $P_b$-type defects are incorporated at the $Si/SiO_2$ interface to account for interfacial stress, which situation will differ for the two cases. Viewed from a different angle, however, should they occur identically in an ordered single Si–O–Al transitional layer, formation of $P_b$-type defects would not require the presence of an $SiO_x$ cap, which then must have repercussions as to the insight in the generation of such defects.

Here, with respect to $Si/SiO_2$, it might be useful to add one more remark. Referring to the very thin transitional layer involved, one might feel tempted to relate the particular $P_{bo}$, $P_{b1}$ character, i.e. broadened signals, enhanced defect densities, as compared to more standard $Si/SiO_2$ ($d_{ox} > 5$ nm) to the ultrasmall thickness of the $SiO_x$-type layer *per se*. However, as outlined previously, the very thickness appears no to be the issue. Rather, what matters is enhanced interfacial stress (unrelaxed state) inherent to low-$T$ fabrication [28].

As probed by the hallmark $P_{bo}$, $P_{b1}$ ESR character, with potential realization of standard low defect densities of (1–1.3) $\times 10^{12}$ cm$^{-2}$, it is thus found that the transition of Si with $ZrO_2$ and $Al_2O_3$ layers may be endowed with the properties of the unsurpassed (100) $Si/SiO_2$ interface: either it may be successfully tailored by deliberately inserting an ultrathin ($\leqslant 0.5$ nm) $SiO_x$ interlayer, or else, as is the case for $Si/Al_2O_3$, it may appear inherently after appropriate postdeposition thermal treatment. The $Si/SiO_2$-type interface is both ultrathin, as required by current demands on low EOT, and of standard $Si/SiO_2$ quality. This apparently natural fact may constitute a fundamental boost for successful application of high-$\kappa$ metal oxides in future Si-based devices. But, of course, besides notorious benefits, the presence of the $Si/SiO_2$-type transition will also pose technological challenges, such as, over the numerous steps in device fabrication, maintaining the interlayer's ultrathin thickness and averting silicide/silicate formation. The latter may result in inferior quality of both interface and dielectric, e.g. introducing an unacceptable density of conduction band tail states [21]. Investigations by NRP and XPS on $Si/Al_2O_3$ indicate that aluminosilicate starts forming under RTA in $O_2$ at $T \geqslant 700$ °C [5]. $ZrO_2$, in contact with Si, becomes thermodynamically unstable under RTA above 900 °C in vacuum or $O_2$ (2 min; 0.1 Torr) [7]. In $Si/SiO_x/ZrO_2$, the $SiO_x$ interlayer thickness is found to increase substantially upon oxidation at 700 °C (15 min) [8].

In summary, paramagnetic defects in (100) $Si/SiO_x/ZrO_2$ and (100) $Si/Al_2O_3/(ZrO_2)$ structures with nm-thin layers grown at 300 °C by the ALCVD method using trimethylaluminium, $ZrCl_4$ and $H_2O$ as precursors, have been probed by ESR. In the as-grown state, there is substantial passivation of defects by hydrogen. After H drive-off, prominent $P_{bo}$, and $P_{b1}$ signals—generally the unique ESR fingerprint of an $Si/SiO_2$ interface—are observed at the Si/insulator interface in all stacks. While suggestively expected for the former structure, it reveals the $Si/Al_2O_3$ interface, in terms of inherent interface defects, also to be basically $Si/SiO_2$ type. It heralds the potential to carrying over of the applauded (100) $Si/SiO_2$ properties towards the Si/metal oxide entities, which may be essential to successful application of high-$\kappa$ metal oxides in technology. In the as-grown state, the spectroscopic properties of the $P_{bo}$,

$P_{b1}$ defects bear out enhanced stress at the pertinent interfaces, inherent to low-$T$ fabrication. Generally, as to the Si/high-$\kappa$ metal oxide structures, the basic ESR story turns out to be another $P_b$-type interface defect saga, where we can beneficially draw upon the immense amount of information assembled for standard thermal $Si/SiO_2$.

## References


[1] See, e.g., Green M, Sorsch T, Timp G, Muller D, Weir B, Silverman P, Moccio S and Kim Y 1999 *Microelectron. Eng.* **48** 25

[2] Lo S H, Buchanan A, Taur Y and Wang W 1997 *IEEE Electron Device Lett.* **18** 209

[3] Lucovsky G *et al* 1999 *Appl. Phys. Lett.* **74** 2005
Lu H C, Yasuda N, Garfunkel E, Chang J P, Opila R L and Alers G 1999 *Microelectron. Eng.* **48** 287

[4] Robertson J 2000 *J. Vac. Sci. Technol.* B **18** 1785

[5] Krug C R, da Rosa E B O, de Almeida R M C, Morais J, Baumvol I J R, Salgado T D M and Stedile F C 2000 *Phys. Rev. Lett.* **85** 4120

[6] Gusev E P, Copel M, Cartier E, Baumvol I J R, Krug C and Gribelyuk M A 2000 *Appl. Phys. Lett.* **76** 176

[7] Copel M, Gribelyuk M and Gusev E 2000 *Appl. Phys. Lett.* **76** 436

[8] Houssa M, Naili M, Zhao C, Bender H, Heyns M M and Stesmans A 2001 *Solid State Commun.* **16** 31

[9] Fukumoto H, Morita M and Osaka Y 1989 *J. Appl. Phys.* **65** 5210

[10] Houssa M, Tuominen M, Naili N, Afanas'ev V, Stesmans A, Haukka S and Heyns M M 2000 *J. Appl. Phys.* **87** 8615

[11] See, e.g., Helms R and Poindexter E H 1998 *Rep. Prog. Phys.* **83** 2449

[12] Bowker K 1988 *Phys. Rev.* B **38** 9657

[13] Poindexter E H 1989 *Semicond. Sci. Technol.* **4** 961

[14] Stesmans A 1993 *Phys. Rev.* B **48** 2418

[15] Stesmans A, Nouwen B and Afanas'ev V 1998 *Phys. Rev.* B **58** 15 801

[16] Stirling A, Pasquarello A, Charlier J-C and Car R 2000 *Phys. Rev. Lett.* **85** 2773

[17] Stesmans A and Afanas'ev V V 1998 *J. Appl. Phys.* **83** 2449

[18] Gabrys J W, Lenahan P M and Weber W 1993 *Microelectron. Eng.* **22** 273

[19] Stesmans A and Afanas'ev V V 1998 *Phys. Rev.* B **57** 10 030

[20] Stesmans A and Afanas'ev V V 1998 *J. Vac. Sci. Technol.* B **16** 3108

[21] Afanas'ev V, Houssa M, Stesmans A and Heyns M 2001 *Appl. Phys. Lett.* **78** 3073

[22] Stesmans A 1996 *Appl. Phys. Lett.* **68** 2076

[23] See, e.g., Griscom D 1958 *J. Appl. Phys.* **58** 2524 and references therein
Edwards A H 1995 *J. Non-Cryst Solids* **187** 232

[24] Pusel A, Wetterauer U and Hess P 1998 *Phys. Rev. Lett.* **81** 645

[25] Brower K L 1986 *Phys. Rev.* B **33** 4471
Stesmans A and Braet J 1986 *Insulating Films on Semiconductors* ed J J Simone and J Buxo (Amsterdam: North-Holland) p 25

[26] Watkins G D and Corbett J W 1964 *Phys. Rev.* **134** A1359

[27] Suntola T 1996 *Appl. Surf. Sci.* **100/101** 391

[28] Stesmans A and Afanas'ev V V 2000 *Appl. Phys. Lett.* **77** 1469